EPJ Web of Conferences **310**, 00015 (2024) https://doi.org/10.1051/epjconf/202431000015
*LNES 2023*

# Microgrids control: AC or DC, that is not the question

Michele Cucuzzella(*) and Jacquelien M. A. Scherpen(**)

*Jan C. Willems Center for Systems and Control, ENTEG, Faculty of Science and Engineering University of Groningen, Nijenborgh 4, 9747 AG Groningen, The Netherlands*

Juan E. Machado(***)

*Brandenburgische Technische Universität, Cottbus-Senftenberg, Germany*

**Summary.** — In these lecture notes, we delve into the models of the most commonly used DC-DC power converters: namely, the buck converter and the boost converter. Furthermore, we derive models for a DC microgrid consisiting of multiple buck and/or boost converters interconnected via (dynamic) resistive-inductive power lines and supplying the so-called ZIP loads, which are characterized by the parallel combination of constant impedance ($Z$), current ($I$), and power ($P$) load components. Furthermore, we introduce the primary control objectives in DC microgrids, focusing on voltage regulation and current sharing. Finally, we explore the most advanced control techniques to achieve these objectives. Importantly, these lecture notes are not intended to advocate total replacement of Alternating Current (AC) power systems with their Direct Current (DC) counterparts, but rather aim to offer a balanced perspective between them, acknowledging the historical dominance of AC power systems while underscoring the contemporary relevance of DC microgrids, which, with their inherent advantages, represent a viable complement to the existing infrastructure, fostering innovation and resilience in modern power networks.

(*) E-mail: m.cucuzzella@rug.nl
(**) E-mail: j.m.a.scherpen@rug.nl
(***) E-mail: machadom@b-tu.de

## 1. – Introduction

In the vast landscape of our modern civilization, few elements are as fundamental and indispensable as electricity. It powers our homes, fuels our industries and drives innovation in all sectors of society. However, as our world evolves, the infrastructure that supports it must also evolve. The emergence of renewable energy sources and the proliferation of power electronics pave the way for a new era in the field of energy production and distribution, in which traditional paradigms are questioned and new solutions are needed [1]. In these lecture notes, we embark on a journey to explore the key role of microgrids in shaping the future of our energy systems, delving into the need for advanced automation and control techniques to address the complexities that lie ahead.

The transition towards renewable energy sources such as solar and wind power represents a paradigm shift in our approach to electricity generation. Unlike their fossil fuel-based counterparts, renewable sources are inherently intermittent and unpredictable, subject to the changes of weather patterns and natural fluctuations. This inherent variability introduces a profound challenge to the stability and reliability of our power grids. Furthermore, the rapid integration of Distributed Energy Resources (DERs), ranging from rooftop solar panels to small-scale wind turbines, adds another layer of complexity, shifting from centralized to decentralized power generation and distribution [1].

Compounding this challenge is the shift away from traditional synchronous generators towards power electronics-based systems. While synchronous generators provide inherent stability to the grid through their rotational inertia, power electronics do not have such inertia, making the system more susceptible to disturbances and fluctuations, exacerbating the issue of grid stability and therefore necessitating a re-evaluation of the existing control strategies and infrastructure [2, 3].

In the face of these challenges, advanced control strategies and algorithms emerge as indispensable tools for a proper grid operation and management. Harnessing the power of cutting-edge technologies such as artificial intelligence, machine learning and advanced sensor networks, intelligent control systems enable real-time monitoring, analysis, and decision-making within the future energy infrastructures. By dynamically adjusting grid parameters, rerouting power flows, and optimizing resource utilization, advanced control systems can mitigate the impact of renewable variability and strengthen the resilience of the grid in the face of uncertainty [4, 5].

For these reasons, in the last decades, motivated by economic, technological and environmental considerations, the primary trajectory of power systems has shifted towards re-configuring conventional power generation and transmission setups to integrate smaller Distributed Generation units (DGus). As a conceptual and technological solution for this evolution, microgrids have emerged, facilitating the integration of various renewable energy sources and the electrification of remote regions. Moreover, by fostering localized resilience and through the integration of renewable energy sources, energy storage systems, and demand response mechanisms, microgrids offer a glimpse into the future of a sustainable and robust energy ecosystem [2, 6].

In the next subsection, we briefly summarize the so-called "War of the Currents" and make some considerations on both Alternating Current (AC) and Direct Current (DC) systems analyzing advantages and disadvantages from a different perspective than that of the 19th century and taking into account the actual changes in our energy system.

**1˙1.** *The war of the currents.* – The "War of the Currents" was a fierce competition between Thomas Edison's DC system and Nikola Tesla and George Westinghouse's AC system during the late 19th century. Edison championed DC, known for its stability but limited transmission range, while Tesla and Westinghouse advocated for AC, which offered efficient long-distance transmission. This rivalry played out through public demonstrations and propaganda campaigns, with Edison attempting to discredit AC by highlighting safety concerns. However, AC's superior transmission capabilities, demonstrated notably through the electrification of the 1893 Chicago World's Fair, led to its widespread adoption as the standard for electrical power systems, marking the victory of the "War of the Currents" and shaping the future of electricity generation and distribution.

Therefore, due to the widespread use of AC electricity in most industrial, commercial, and residential applications, the literature on microgrids mainly focused on AC microgrids [4,7-14]. However, nowadays the actual power system is very different than it was in the 19th century, evolving towards a landscape characterized by an increasing integration of diverse energy sources and loads, where DC microgrids can offer several advantages over the AC counterparts (see, *e.g.*, [15] and the references therein).

A key advantage lies in the fact that nowadays several sources and loads such as photovoltaic panels, fuel cells, batteries, electric vehicles and many other electronic appliances (see figs. 1 and 2), can be directly connected to DC microgrids through DC-DC power converters. Unlike in AC grids, where conversion to AC is often necessary, DC microgrids allow for a seamless integration of various sources and loads without the inefficiencies associated with multiple conversions. This simplicity not only enhances overall system efficiency but also reduces the complexity and cost of infrastructure. Remarkably, DC microgrids offer a greater flexibility in accommodating renewable energy sources such as solar panels, which naturally generate DC power. Figure 1 shows a simple but very clear example of how interconnecting certain sources and loads through a DC network is much more advantageous than interconnecting them through an AC network. Specifically, an AC distribution system requires many more power converters than a DC one, implying a more complex and expensive infrastructure as well as a less efficient system due to the larger conversion stages.

Moreover, the growing need of interconnecting distant power networks (*e.g.* off-shore wind farms) has encouraged the use of High Voltage Direct Current (HVDC) technology, which is advantageous not only for long distances, but also for underwater cables, asynchronous networks and grids running at different frequencies [16]. Finally, DC microgrids are currently investigated to be widely deployed in aircrafts and trains, and recently used in modern design for ships, large charging facilities for electric vehicles, and data centers (see fig. 2).

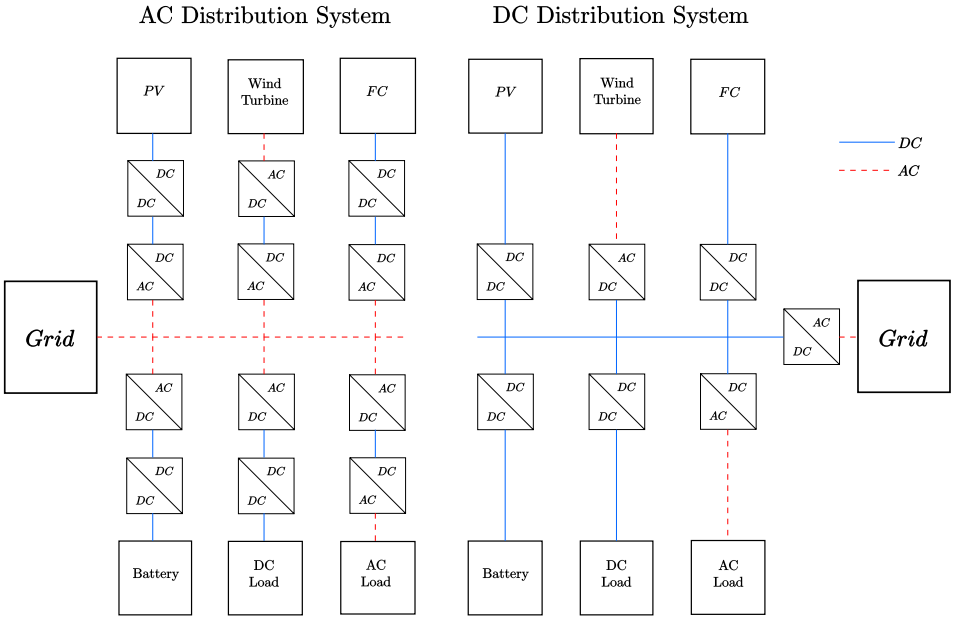


Fig. 1. – Comparison between AC and DC infrastructures interconnecting certain devices.

Fig. 2. – Examples of DC microgrids.

The advantages of DC networks over AC networks discussed above, along with others, are summarized in the following:

- fewer DC-AC and AC-DC conversion stages increase efficiency and reduce complexity, losses, and infrastructure costs;
- not having to control the reactive power and not having to adjust the frequency simplify the control design and increase the power system reliability;
- the absence of harmonics and the notorious skin effect increases the system power quality.

Therefore, as the energy transition progresses, the scalability and adaptability of DC microgrids position them favorably for supporting distributed generation and enhancing grid resilience in the future electricity system. For all these reasons, DC microgrids are attracting growing interest and receive much research attention.

**1**˙2. *Outline*. – In these lecture notes we present in sect. **2** the models of the most common used DC-DC power converters: the buck converter and the boost converter. We also derive the models of a DC microgrid comprising several buck and/or boost converters interconnected with each other through (dynamic) resistive-inductive power lines and supplying the so-called ZIP loads, *i.e.*, nonlinear loads consisting of the parallel combination of constant impedance ($Z$), current ($I$) and power ($P$) load components. In sect. **3**, we will introduce the main control objectives in DC microgrids: voltage regulation and current sharing. In sect. **4**, we will discuss the main control techniques to achieve these objectives in both buck and boost converter-based DC microgrids. Some conclusions are finally gathered in sect. **5**.

**1**˙3. *Notation*. – The set of (positive) real numbers is denoted by $(\mathbb{R}_{>0})\,\mathbb{R}$. Let $\mathbf{0}$ be the vector of all zeros of suitable dimension and let $\mathbb{1}_n \in \mathbb{R}^n$ be the vector containing all ones. The $i$-th element of a vector $x$ is denoted by $x_i$. A steady state solution to system $\dot{x} = f(x)$, is denoted by $\overline{x}$, *i.e.*, $\mathbf{0} = f(\overline{x})$. Let "$\circ$" denote the Hadamard product, *i.e.*, given vectors $x, y \in \mathbb{R}^n$, $(x \circ y) \in \mathbb{R}^n$ is a vector with elements $(x \circ y)_i := x_i y_i$ for all $i = 1, \ldots, n$. For notation simplicity, when it is obvious from the context, the dependence of the variables on time $t$ is omitted throughout these lecture notes.

## 2. – Models of DC microgrids

In this section, we introduce the models of the most widespread DC-DC power converters: the buck and boost converters, which describe in form and function a large family of DC-DC power converters [17]. Moreover, we present the models of a network of buck converters, a network of boost converters, and a network of both buck and boost converters interconnected with each other through (dynamic) resistive-inductive power lines.

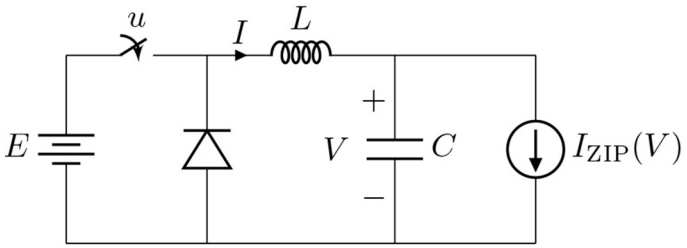


Fig. 3. – Electrical scheme of a buck converter supplying a ZIP load.

**2**˙1. *Buck converter-based DC microgrid.* – A buck converter, also known as a step-down converter, is a type of DC-to-DC converter designed to decrease the voltage, while increasing the current from its input (supply) to its output (load). This device belongs to the category of switched-mode power converters.

Consider the electrical scheme of a buck converter in fig. 3, where $E > 0$ denotes a (current-controlled) voltage source, $u \in \{0, 1\}$ indicates the state of the switch, *i.e.*, "open" or "close", $I(t) \in \mathbb{R}$ denotes the current through the inductor $L$, and $V(t) \in \mathbb{R}_{>0}$ denotes the voltage across the capacitor $C$. Moreover, $I_{\mathrm{ZIP}}(V) > 0$ denotes the current absorbed by a ZIP load, *i.e.*, a nonlinear load consisting of the parallel combination of constant impedance ($Z$), current ($I$) and power ($P$) load components (see fig. 4).

One of the most widely utilized techniques for opening and closing the switch(es) of power converters is the well-known pulse width modulation (PWM) technique, which varies the duty cycle of the converter switch(es) at a high switching frequency to achieve a target average low-frequency output voltage or current.

Under the reasonable assumption that the PWM switching frequency is sufficiently high, the switching control input can be replaced by the so-called "duty cycle" of the converter [18]. Therefore, we will consider in the following the "average" inductor current and the "average" capacitor voltage. With a slight abuse of notation, but for the sake of simplicity, from now on, let $I$, $V$, and $u \in [0, 1]$ denote, respectively, the average signals (in a given period) of the current through the inductor, the voltage across the capacitor, and the switching control signal.

Now, let assume the diode to be ideal. Then, by applying Kirchhoff's current and voltage laws, the average governing dynamic equations of the buck converter are the following (see, *e.g.*, [19]):

$$\begin{aligned} L\dot{I} &= -V + uE, \\ C\dot{V} &= I - I_{\mathrm{ZIP}}(V), \end{aligned} \tag{1}$$

where the current absorbed by the ZIP load represented in fig. 4 is given by (see, *e.g.*, [20])

$$I_{\mathrm{ZIP}}(V) = Z^{*-1}V + I^* + \frac{P^*}{V}\,, \tag{2}$$

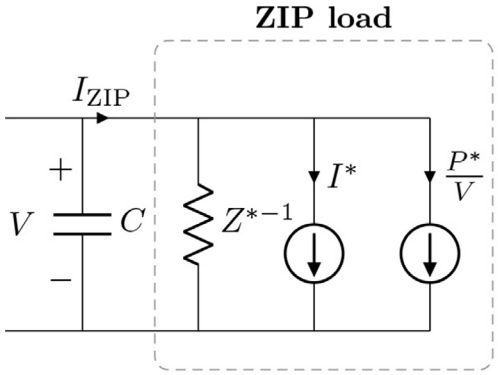


Fig. 4. – Electrical scheme of a ZIP load, *i.e.*, a nonlinear load consisting of the parallel combination of constant impedance ($Z$), current ($I$) and power ($P$) load components.

with $Z^* > 0$, $I^* > 0$, and $P^* > 0$ denoting the constant impedance, current and power components of the ZIP load in fig. 4.

Now, we consider a typical buck converter-based DC microgrid composed of $n$ DGUs connected to each other through $m$ resistive-inductive power lines (see fig. 5 for a schematic electrical diagram of a DC microgrid composed of two DGUs and a resistive-inductive power line). Following steps similar to those above, by applying the Kirchhoff's current and voltage laws, the average governing dynamic equations of the $i$-th DGU are the following (see, *e.g.*, [19]):

$$\begin{aligned} L_i \dot{I}_i &= -V_i + u_i E_i, \\ C_i \dot{V}_i &= I_i - I_{\text{ZIP},i}(V_i) - \sum_{k \in \mathcal{E}_i} I_{l,k}, \end{aligned} \tag{3}$$

where $\mathcal{E}_i$ denotes the set of the power lines incident to the $i$-th DGU, while all the other symbols have the same meaning as in (1) (see also fig. 5 for a better understanding). Moreover, in (3) and in fig. 5, $I_{l,k}$ denotes the current from DGU $i$ to DGU $j \neq i$, and its dynamics are given by

$$L_{l,k} \dot{I}_{l,k} = (V_i - V_j) - R_{l,k} I_{l,k}, \tag{4}$$

where $I_{l,k}(t) \in \mathbb{R}$ denotes the current through the inductor $L_{l,k}$ of the resistive-inductive power line $k$, $V_i(t) \in \mathbb{R}_{>0}$ and $V_j(t) \in \mathbb{R}_{>0}$ denote the voltages across the capacitors $C_i$ and $C_j$, respectively. Furthermore, $R_{l,k}$ denotes the resistance of the power line $k$.

The overall DC power network can be represented by a connected and (oriented) undirected graph $\mathcal{G} = (\mathcal{V}, \mathcal{E})$, where $\mathcal{V} = \{1, \ldots, n\}$ represents the set of the nodes (*i.e.*, the DGUs), and $\mathcal{E} = \{1, \ldots, m\}$ represents the set of the edges (*i.e.*, the power lines interconnecting the DGUs). The network topology is described by its corresponding

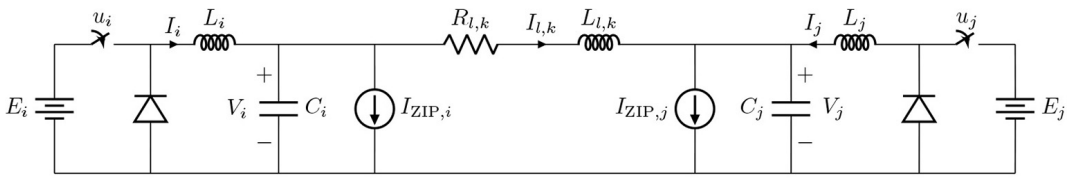


Fig. 5. – Electrical scheme of a DC microgrid composed of two buck converters interconnected through a resistive-inductive power line and supplying two ZIP loads.

incidence matrix $B \in \mathbb{R}^{n\times m}$. The ends of an edge $k$ are arbitrarily labeled with a $+$ and a $-$, and the entries of $B$ are given by

$$B_{ik} = \begin{cases} +1 & \text{if } i \text{ is the positive end of } k, \\ -1 & \text{if } i \text{ is the negative end of } k, \\ 0 & \text{otherwise.} \end{cases} \tag{5}$$

Consequently, the overall microgrid average dynamics can be written compactly for all DGUs $i \in \mathcal{V}$ as (see, *e.g.*, [19])

$$\begin{aligned} L\dot{I} &= -V + E \circ u, \\ C\dot{V} &= I + BI_l - I_{\mathrm{ZIP}}(V), \\ L_l\dot{I}_l &= -B^\top V - R_l I_l, \end{aligned} \tag{6}$$

where, with a slight abuse of notation, $I(t)$, $V(t)$, $I_{\mathrm{ZIP}}(V)$, $u(t)$, $E \in \mathbb{R}^n$, and $I_l(t) \in \mathbb{R}^m$ denote the vectors stacking the corresponding variables of all the nodes and edges, respectively, *e.g.*, $I = [I_1, \cdots, I_n]^\top$. Moreover, $C, L \in \mathbb{R}^{n\times n}$ and $R_l, L_l \in \mathbb{R}^{m\times m}$ are positive definite diagonal matrices, *e.g.*, $C = \mathrm{diag}(C_1, \ldots, C_n)$.

**2**˙2. *Boost converter-based DC microgrid*. – A boost converter, also known as a step-up converter, is a type of DC-to-DC converter designed to increase the voltage, while decreasing the current from its input (supply) to its output (load). Like the buck converter, also the boost converter belongs to the category of switched-mode power converters.

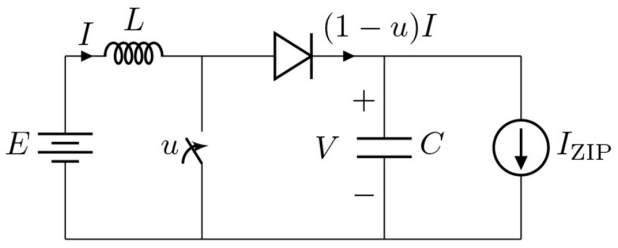


Fig. 6. – Electrical scheme of a boost converter supplying a ZIP load.

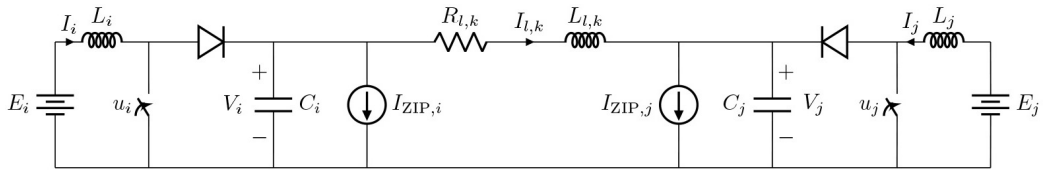


Fig. 7. – Electrical scheme of a DC microgrid composed of two boost converters interconnected through a resistive-inductive power line and supplying two ZIP loads.

Consider the electrical scheme of a boost converter in fig. 6, where the description of each electrical component and variable is the same as for the buck converter dynamics (1) in subsect. **2**˙1.

Now, let the PWM switching frequency be sufficiently high and let the diode to be ideal. Then, by applying the Kirchhoff's current and voltage laws, the average governing dynamic equations of the boost converter are the following (see, *e.g.*, [19])

$$\begin{aligned} L\dot{I} &= -(1-u)V + E, \\ C\dot{V} &= (1-u)I - I_{\mathrm{ZIP}}(V), \end{aligned} \tag{7}$$

where the current absorbed by the ZIP load represented in fig. 4 is given by (2).

Now, similarly to subsect. **2**˙1, we consider a typical boost converter-based DC microgrid composed of $n$ DGUs connected to each other through $m$ resistive-inductive power lines (see fig. 7 for a schematic electrical diagram of a DC microgrid composed of two DGUs and a resistive-inductive power line). By applying the Kirchhoff's current and voltage laws, the average governing dynamic equations of the $i$-th DGU are the following (see, *e.g.*, [19]):

$$\begin{aligned} L_i\dot{I}_i &= -(1-u_i)V_i + E_i, \\ C_i\dot{V}_i &= (1-u_i)I_i - I_{\mathrm{ZIP},i}(V_i) - \sum_{k\in\mathcal{E}_i} I_{l,k}, \end{aligned} \tag{8}$$

where all the symbols have the same meaning as for the buck converter (1) in subsect. **2**˙1 (see also fig. 7 for a better understanding). Moreover, in (8) and in fig. 7, $I_{l,k}$ denotes the current from DGU $i$ to DGU $j \neq i$, and its dynamic is given by (4).

Recalling from subsect. **2**˙1 that the overall DC power network can be represented by a connected and (oriented) undirected graph $\mathcal{G} = (\mathcal{V}, \mathcal{E})$, where $\mathcal{V} = \{1, \ldots, n\}$ denotes the set of the DGUs, and $\mathcal{E} = \{1, \ldots, m\}$ denotes the set of the power lines interconnecting the DGUs, the overall microgrid average dynamics can be written compactly for all DGUs $i \in \mathcal{V}$ as (see, *e.g.*, [19])

$$\begin{aligned} L\dot{I} &= -(\mathbb{1}_n - u) \circ V + E, \\ C\dot{V} &= (\mathbb{1}_n - u) \circ I + BI_l - I_{\mathrm{ZIP}}(V), \\ L_l\dot{I}_l &= -B^\top V - R_l I_l, \end{aligned} \tag{9}$$

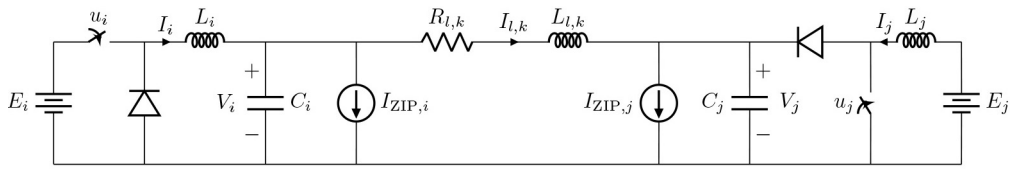


Fig. 8. – Electrical scheme of a DC microgrid composed of a buck and a boost converter interconnected through a resistive-inductive power line and supplying two ZIP loads.

where, with a slight abuse of notation, $I(t)$, $V(t)$, $I_{\mathrm{ZIP}}(V)$, $u(t)$, $E \in \mathbb{R}^n$, and $I_l(t) \in \mathbb{R}^m$ denote the vectors stacking the corresponding variables of all the nodes and edges, respectively, *e.g.*, $I = [I_1, \cdots, I_n]^\top$. Moreover, $C, L \in \mathbb{R}^{n\times n}$ and $R_l, L_l \in \mathbb{R}^{m\times m}$ are positive definite diagonal matrices, *e.g.*, $C = \mathrm{diag}(C_1, \ldots, C_n)$, while $B$ denotes the incidence matrix describing the network topology and is defined in (5).

**2**˙3. *Buck and boost converter-based DC microgrid.* – In this subsection we consider a typical DC microgrid of which a schematic electrical diagram is provided in fig. 8, including both buck and boost DC-DC power converters interconnected through resistive-inductive power lines. In the following we adopt the subscripts $\alpha$ or $\beta$ in order to refer to the buck or boost type converter, respectively. The microgrid is composed of $n$ DGUs of which $n_\alpha$ have a buck converter and $n_\beta$ have a boost converter, *i.e.*, $n_\alpha + n_\beta = n$. The DGUs are interconnected to each other through $m$ resistive-inductive power lines. Therefore, the average governing dynamic equations of the DGU $i \in \mathcal{V}_\alpha$ are given by (3), those of the DGU $i \in \mathcal{V}_\beta$ are given by (8), and the current dynamics from DGU $i$ to DGU $j \neq i$ are given by (4).

Now, we represent the overall DC power network by a connected and (oriented) undirected graph $\mathcal{G} = (\mathcal{V}_\alpha \cup \mathcal{V}_\beta, \mathcal{E})$, where $\mathcal{V}_\alpha = \{1, \ldots, n_\alpha\}$ denotes the set of the DGUs with buck converters, $\mathcal{V}_\beta = \{n_\alpha + 1, \ldots, n\}$ denotes the set of the DGUs with boost converters, and $\mathcal{E} = \{1, \ldots, m\}$ denotes the set of the power lines interconnecting the DGUs. The network topology can be described by its corresponding incidence matrix $B \in \mathbb{R}^{n\times m}$ (see (5)), and therefore the overall microgrid average dynamics can be written compactly for all DGUs $i \in \mathcal{V}_\alpha \cup \mathcal{V}_\beta$ as (see, *e.g.*, [19])

$$
\begin{aligned}
L_\alpha \dot{I}_\alpha &= -V_\alpha + E_\alpha \circ u_\alpha, \\
L_\beta \dot{I}_\beta &= -(\mathbb{1}_{n_\beta} - u_\beta) \circ V_\beta + E_\beta, \\
L_l \dot{I}_l &= -B^\top V - R_l I_l, \\
C_\alpha \dot{V}_\alpha &= I_\alpha + B_\alpha I_l - I_{\mathrm{ZIP},\alpha}(V_\alpha), \\
C_\beta \dot{V}_\beta &= (\mathbb{1}_{n_\beta} - u_\beta) \circ I_\beta + B_\beta I_l - I_{\mathrm{ZIP},\beta}(V_\beta),
\end{aligned}
\tag{10}
$$

where $I_\alpha(t)$, $V_\alpha(t)$, $I_{\mathrm{ZIP},\alpha}(V_\alpha)$, $u_\alpha(t)$, $E_\alpha \in \mathbb{R}^{n_\alpha}$, $I_\beta(t)$, $V_\beta(t)$, $I_{\mathrm{ZIP},\beta}(V_\beta)$, $u_\beta(t)$, $E_\beta \in \mathbb{R}^{n_\beta}$, $I_l \in \mathbb{R}^m$. Moreover, $L_\alpha$, $L_\beta$, $L_l$, $C_\alpha$, $C_\beta$, $R_l$ are positive definite diagonal matrices

of appropriate dimensions. The matrices $B_\alpha \in \mathbb{R}^{n_\alpha \times m}$ and $B_\beta \in \mathbb{R}^{n_\beta \times m}$ are obtained by collecting from $B$ the rows indexed by $\mathcal{V}_\alpha$ and $\mathcal{V}_\beta$, respectively.

## 3. – Control objectives in DC microgrids

From now on we focus only on the buck converter-based DC microgrid (6) introduced in subsect. **2**˙1, and on the boost converter-based DC microgrid (9) introduced in subsect. **2**˙2. Specifically, in this section we formulate and explain the main control objectives in DC microgrids, *i.e.*, voltage regulation and current sharing (or, equivalently, load sharing). Regulating voltages is essential to ensure a proper functioning of the connected electrical devices, such as the loads [19-33], while current sharing prevents any source from being overstressed [31,34-47]. Additionally, as microgrids may include DGUs with different generation capacity, achieving proportional current sharing among them is often desired in practice. This ensures that each DGU contributes to the total current demand in proportion to its generation capacity, a concept known as "proportional" current sharing. Generally, achieving current sharing limits the ability to regulate the voltage at each node towards a corresponding desired value. Then, a reasonable alternative is to satisfy the voltage requirements outlined in [48], which suggests to regulate the average voltage across the entire microgrid, rather than specific nodes, to meet a global voltage set point (*e.g.*, the average of the voltage references). This method, known as global voltage regulation or voltage balancing, has been discussed in prior research (see, for instance, [35, 43-45] and the references therein).

**3**˙1. *Voltage regulation.* – In the following, we introduce the voltage regulation objective, that is to regulate the voltage across the loads to a desired reference value.

*Objective 1 (Voltage regulation).*

$$\lim_{t\to\infty} V_i(t) = \overline{V}_i = V_i^*, \quad \forall i \in \mathcal{V}, \tag{11}$$

*where $V_i^* \in \mathbb{R}_{>0}$ is the desired value for the voltage $V_i$ of node $i \in \mathcal{V}$.*

Note that, in the case of a buck converter-based DC microgrid (6) (see subsect. **2**˙1), the desired voltage value satisfies $V_i^* < E_i$ for all $i \in \mathcal{V}$. On the other hand, in the case of a boost converter-based DC microgrid (9) (see subsect. **2**˙2), the desired voltage value satisfies $V_i^* > E_i$ for all $i \in \mathcal{V}$.

**3**˙2. *Current sharing and voltage balancing.* – Since the majority of the existing literature on current sharing mainly focuses on buck converter-based DC microgrids, these lecture notes also delve into the current sharing objective for a DC microgrid (6).

As discussed above, in order to avoid the overstressing of a source and to improve the generation efficiency, it is generally desired that the total demand of the network, *i.e.*, $\mathbb{1}_n^\top I_{\mathrm{ZIP}}(V)$, is shared among all the various DGUs proportionally to the generation capacity of their corresponding energy sources and/or storage devices (proportional

current sharing). Then, the proportional current sharing objective can be formulated as $w_i\overline{I}_i = w_j\overline{I}_j$ for all $i, j \in \mathcal{V}$, where a relatively large value of $w_i$ corresponds to a relatively small generation capacity of the DGU $i$. This leads to the following control objective, concerning with the steady state value of the output currents $\overline{I}_i$ for each buck converter $i \in \mathcal{V}$.

*Objective 2 (Current sharing).*

$$\lim_{t\to\infty} I(t) = \overline{I} = W^{-1}\mathbb{1}_n i^*, \tag{12}$$

*with* $W = \mathrm{diag}(w_1, \ldots, w_n)$, $w_i > 0$, *for all* $i \in \mathcal{V}$ *and* $i^*$ *defined as*

$$i^* = \frac{\mathbb{1}_n^\top I_{\mathrm{ZIP}}(\overline{V})}{\mathbb{1}_n^\top W^{-1}\mathbb{1}_n}. \tag{13}$$

To better understand the current sharing objective, first we notice that for a given input $\overline{u}$, a steady state solution $(\overline{I}, \overline{V}, \overline{I}_l)$ to (6) satisfies

$$\overline{V} = \overline{u}, \tag{14a}$$
$$I_{\mathrm{ZIP}}(\overline{V}) - \overline{I} = B\overline{I}_l, \tag{14b}$$
$$\overline{I}_l = -R_l^{-1}B^\top\overline{V}. \tag{14c}$$

Equation (14b) implies([1]) that at the steady state the total generated current $\mathbb{1}_n^\top\overline{I}$ is indeed equal to the total current demand $\mathbb{1}_n^\top I_{\mathrm{ZIP}}(\overline{V})$. Therefore, we can conclude that the steady-state equality $\mathbb{1}_n^\top\overline{I}_t = \mathbb{1}_n^\top I_L$ necessarily prescribes that $i^*$ in (12) is given by (13). Furthermore, we can observe that achieving Objective 2 does not permit in general to attain simultaneously also Objective 1, *i.e.*, $\overline{V} = V^*$. Specifically, equations (14b) and (14c) impose that the steady-state voltage $\overline{V}$ satisfies $BR_l^{-1}B^\top\overline{V} = W^{-1}\mathbb{1}_n i^* - I_{\mathrm{ZIP}}(\overline{V})$. However, this allows for the adjustment of all steady-state voltages by the same constant value, since $B^\top\overline{V} = B^\top(\overline{V} + a\mathbb{1}_n)$, with $a \in \mathbb{R}$ any scalar. We therefore aim at an *average voltage regulation*, where the weighted average value of $\overline{V}$ is identical to the weighted average value of the desired reference voltages $V^\star$. Following the standard practice in which the sources with the highest generation capacity determine the grid voltage, we select a weight of $\frac{1}{w_i}$ for all $i \in \mathcal{V}$, leading to the following objective.

*Objective 3 (Voltage balancing).*

$$\lim_{t\to\infty} \mathbb{1}_n^\top W^{-1}V(t) = \mathbb{1}_n^\top W^{-1}\overline{V} = \mathbb{1}_n^\top W^{-1}V^*. \tag{15}$$

([1]) The incidence matrix $B$, satisfies $\mathbb{1}_n^\top B = \mathbf{0}$.

## 4. – Control of DC microgrid: a review

In this section we review some of the most advanced decentralized([2]) control schemes to achieve voltage regulation (Objective 1) in both buck and boost converter-based DC microgrids (see (6) and (9), respectively). Finally, we review some of the most advanced distributed([3]) control schemes to achieve current sharing (Objective 2) and voltage balancing (Objective 3) in a buck converter-based DC microgrid (6).

**4**˙1. *Voltage regulation in buck converter-based DC microgrids.* – In order to achieve Objective 1 for a buck converter-based DC microgrid (6), several controllers based on different approaches have been proposed in the last decades for the case where constant power loads are not considered (*i.e.*, $P = 0$). These include for example droop [21], plug-and-play [49, 50], sliding mode [42] and energy-based [17, 19] controllers. Then, in order to address the destabilizing effect of $P$-loads, energy-based approaches have been developed in the last few years (see for example [26, 51, 52]). However, restrictive (sufficient) conditions on the load parameters ($Z$ and $P$), voltage trajectory and voltage reference are assumed to be satisfied or the knowledge of some system parameters is required. Some of these conditions have been relaxed in [29], where however the control law uses the voltage derivative, thus loosing robustness with respect to noisy voltage measurements. Additionally, in all these works, stability is ensured only under the assumption that each component of the ZIP-loads is *constant*, while in practice these parameters are evidently time-varying. In [27, 28] time-varying loads are included in the analysis, yet, an underlying assumption within these works is that the loads are defined from known exosystems, which might not be the case in some applications.

Now, we briefly present the fully decentralized control scheme proposed in [20]. Following the notation used in these lecture notes, the controller proposed in [20] can be rewritten for the node $i \in \mathcal{V}$ as

$$\dot{x}_{c,i} = -k_{1,i}(V_i - V_i^*) - k_{2,i} I_i - k_{3,i} x_{c,i}, \tag{16a}$$

$$v_i = -k_{4,i}(V_i - V_i^*) - k_{5,i} I_i - k_{6,i} x_{c,i}, \tag{16b}$$

$$E_i u_i = V_i^* + v_i, \tag{16c}$$

where the gains $k_{1,i}, \dots, k_{6,i} \in \mathbb{R}$ are suitable constants (see [20, eq. (19)] for more details on how to select the controller gains), while $x_{c,i}$ is the state of the controller at the node $i \in \mathcal{V}$.

The rationale behind the controller (16) is the following. The feed-forward control (16c) simply sets the nominal voltage for the DC microgrid (6). In the absence

([2]) We say that a controller is decentralized if it does not require information about other controllers or DGUs.
([3]) We say that a controller is distributed if it requires information only about the neighbouring controllers or DGUs. This is contrast to a centralized control scheme, which requires information about all the DGUs of the microgrid.

of losses or loads, this control action would be sufficient to regulate the network voltage. However, due to the presence of uncertain loads, we consider an additional control input $v_i$ to design a feedback controller ensuring that the voltage of the $i$-th DGU is stabilised at the desired voltage level $V_i^*$. The controller (16a), (16b) has two key properties. Firstly, a dissipative term is added into the voltage coordinates that is used to tune the region of stability of the network. Secondly, a dynamic state is included in the controller which acts as an integrator on the network voltage error, ensuring that the voltage converges to the nominal set-point whilst rejecting the effects of unknown loads (unmatched disturbances). Then, we say that the controller (16) is "robust" against load uncertainty.

Increasing the region of stability is the major advantage of the controller (16) compared to the existing literature, where network stability is predominantly constrained by the positivity of the equivalent load conductance (*i.e.*, the conductance corresponding to the parallel connection of $Z$- and $P$-loads) at each DGU (see [26,51]), which however leads to restrictive conditions on load parameters, voltage trajectories, and references, limiting the stability region of existing control strategies, especially for high-impedance loads and low-voltage microgrids. To the best of our knowledge, (16) is the first controller to relax the requirement regarding the positivity of the equivalent conductance. Specifically, the proposed controller ensures the damping structure of the closed-loop system is positive definite over a relatively large region of the state space. In the absence of time-varying disturbances, the DC network exhibits an exponentially stable desired equilibrium, whose stability region can be adjusted by tuning the controller gains. When subjected to arbitrary bounded time-varying disturbances, the closed-loop system demonstrates local input-to-state stability [53].

All the details about the stability analysis of a DC microgrid (6) in closed loop with (16) can be found in [20], together with extensive simulation scenarios.

**4˙2.** *Voltage regulation in boost converter-based DC microgrids.* – In order to achieve Objective 1 for a boost converter-based DC microgrid (9), several controllers based on different approaches have been proposed in the last decades for the case where constant power loads are not considered (*i.e.*, $P = 0$) and/or the line dynamics are neglected (*i.e.*, $L_l = 0$). These includes for example passivity-preserving [17] and plug-and-play [49] controllers.

Now, we briefly present the fully decentralized control scheme proposed in [19, 25]. Following the notation used in these lecture notes, the controller proposed in [19, 25] can be rewritten for the node $i \in \mathcal{V}$ as

$$\dot{u}_i = -k_{1,i}(u_i - u_i^*) - k_{2,i}\left(\dot{I}V - \dot{V}I\right), \tag{17}$$

where $u_i^* = 1 - E_i^*/V_i^*$ is the desired value of the duty-cycle of the boost converter $i \in \mathcal{V}$, whose expression can be obtained from the first equation of (8) at the steady state and it depends only on the voltage source $E_i$ and the desired voltage value $V_i^*$ of node $i \in \mathcal{V}$. Moreover, $k_{1,i}, k_{2,i} \in \mathbb{R}_{>0}$ are the controller gains, whose values affect only the transient performance of (9) in closed loop with the decentralized controller (17) and they can be

tuned depending on the particular application and desired performance.

The controller (17) belongs to the class of passivity-based controllers and, specifically, it is called "input-shaping" controller [19], since the control input $u$ is used to shape the equilibrium of the closed-loop system (9), (17) at the desired operating point $(\overline{I}, V^*, \overline{I}_l, u^*)$, where $u_i = u_i^*$ and $V_i = V_i^*$ for all $i \in \mathcal{V}$, achieving Objective 1.

Differently from the majority of controllers reported in the literature, the controller (17) is robust with respect to unknown loads and other parameter uncertainty (*e.g.*, line and filter impedance). Furthermore, besides considering the nonlinear nature of the boost converter and resistive-inductive lines, the controller (17) provides theoretical (local) stability guarantees also in presence of ZIP loads (2).

All the details about the stability analysis of a DC microgrid (9) in closed loop with (17) can be found in [19, 25], together with extensive experiments on a real DC microgrid test facility.

**4˙3.** *Current sharing and voltage balancing in buck converter-based DC microgrids.* – In order to achieve Objectives 2 and 3 for a buck converter-based DC microgrid (6), several controllers based on different approaches have been proposed [31, 34-47].

Now, we briefly present the fully distributed control scheme proposed in [41,46]. First, we assume that there is a connected, undirected —and weighted— communication graph $\mathcal{G}^{\text{com}} = (\mathcal{V}^{\text{com}}, \mathcal{E}^{\text{com}}, \Gamma^{\text{com}})$ involving all DGUs, *i.e.*, $\mathcal{V}^{\text{com}} = \mathcal{V}$. However, $\mathcal{G}^{\text{com}}$ does not have (necessarily) the same topology of the microgrid graph $\mathcal{G}$, *i.e.*, $\mathcal{E}^{\text{com}}$ can differ from $\mathcal{E}$. Following the notation used in these lecture notes, the controller proposed in [41, 46] can be rewritten for the node $i \in \mathcal{V}$ as

$$
\begin{aligned}
k_{1,i}\dot{\theta}_i &= -\sum_{j \in \mathcal{N}_i^{\text{com}}} \gamma_{ij}(w_i I_i - w_j I_j), \\
k_{2,i}\dot{\phi}_i &= -\phi_i + I_i, \\
u_i &= -k_{3,i}(I_i - \phi_i) + w_i \sum_{j \in \mathcal{N}_i^{\text{com}}} \gamma_{ij}(\theta_i - \theta_j) + V_i^*,
\end{aligned}
\tag{18}
$$

where, the gains $k_{1,i}, \ldots, k_{3,i} \in \mathbb{R}_{>0}$ permit an appropriate tuning of the transient performance, while $\mathcal{N}_i^{\text{com}}$ is the set of nodes connected to node $i$ via communication links, with edge weights $\gamma_{ij} = \gamma_{ji} \in \mathbb{R}_{>0}$. Therefore, the controller (18) is distributed as it exchanges information about $I$ and $\theta$ among the neighbouring nodes. Similarly to the topology of the microgrid, the communication network topology is described by its corresponding incidence matrix $B^{\text{com}} \in \mathbb{R}^{n \times m_c}$, which is defined similarly as $B$ in (5). Then, the overall control scheme can be compactly written for all $i \in \mathcal{V}$ as

$$K_1\dot{\theta} = -L^{\text{com}} W I, \tag{19a}$$

$$K_2\dot{\phi} = -\phi + I, \tag{19b}$$

$$u = -K_3(I - \phi) + W L^{\text{com}}\theta + V^*, \tag{19c}$$

where $K_1, \ldots, K_3 \in \mathbb{R}^{n\times n}$ are positive definite diagonal matrices, and the matrix $L^{\mathrm{com}} = B^{\mathrm{com}}(B^{\mathrm{com}})^\top$ is a (weighted) Laplacian associated with $\mathcal{G}^{\mathrm{com}}$.

The rationale behind the controller (19) is the following. First, we observe that (19$a$) is a consensus dynamics and the generated current at the equilibrium necessarily satisfies $W\bar{I} \in \mathcal{R}(\mathbb{1})$, with $\mathcal{R}(\mathbb{1})$ denoting the range of $\mathbb{1}$, *i.e.*, all elements of $W\bar{I}$ are identical (see Objective 2). The dynamics (19$b$) acts as a filter on $I$ and the term $-K(I_{\mathrm{g}} - \phi)$ in (19$c$) does not change the desired equilibrium value, but it was shown in [36, 41, 46] to be very useful in practice to attenuate oscillations during transients. Finally, the term $WL^{\mathrm{com}}\theta + V^*$ in (19$c$) stems from the desire to establish a *passive* interconnection with the state $\theta$ and simultaneously address Objective 3. Indeed, in closed-loop, the steady-state relation $-\bar{V} + WL^{\mathrm{com}}\bar{\theta} + V^* = 0$ holds, which after pre-multiplication by $\mathbb{1}^\top W^{-1}$ leads to (15).

All the details about the stability analysis of a DC microgrid (6) in closed loop with (19) can be found in [41, 46], together with extensive simulation scenarios and experiments on a real DC microgrid test facility [36]. Moreover, in the case DGUs are affected by unknown and potentially time-varying parasitic resistances, in [54] it has been proposed to equip the control scheme (19) with a sliding mode observer to estimate the parasitic resistance. As an alternative, a distributed adaptive control scheme based on back-stepping and passivity theory has been developed.

*Remark 1. Note that achieving current sharing while preserving the average voltage of the network may not always be desired, as it may introduce, in some nodes of the microgrid, large voltage deviations from the corresponding desired value. Consider for instance a DC microgrid with 2 DGUs interconnected through a purely resistive transmission line, the value of which is relatively large (e.g., because the two nodes are spatially distant). Moreover, assume that the load demand of one of the DGUs is much higher than the other. Then, in order to achieve current sharing, the DGUs need to share a relatively large current through the transmission line, implying a relatively large voltage deviation (with respect to the desired value). Then, a steady-state solution satisfying* (12) *and* (15) *may be not feasible in practical applications. To address this problem, distributed feedback controllers solving an optimization problem (including e.g. voltage constraints) have been proposed in* [55-57].

## 5. – Conclusions

In summary, these lecture notes explore the models of the most used DC-DC power converters, including the buck and boost converters. Additionally, we analyze the models for DC microgrids comprising multiple interconnected buck and/or boost converters supplying ZIP loads. Moreover, the primary control objectives in DC microgrids, namely voltage regulation and current sharing, are introduced together with advanced control techniques to achieve them.

REFERENCES

[1] Puttgen H., MacGregor P. and Lambert F., "Distributed generation: Semantic hype or the dawn of a new era?," *IEEE Power Energy Mag.*, **1** (2003) 22.
[2] Massoud Amin S. and Wollenberg B., "Toward a smart grid: power delivery for the 21st century," *IEEE Power Energy Mag.*, **3** (2005) 34.
[3] Carrasco J., Franquelo L., Bialasiewicz J., Galvan E., PortilloGuisado R., Prats M., Leon J. and Moreno-Alfonso N., "Power-electronic systems for the grid integration of renewable energy sources: A survey," *IEEE Trans. Indust. Electron.*, **53** (2006) 1002.
[4] Guerrero J. M., Loh P. C., Lee T.-L. and Chandorkar M., "Advanced control architectures for intelligent microgrids—part ii: Power quality, energy storage, and AC/DC microgrids," *IEEE Trans. Indust. Electron.*, **60** (2013) 1263.
[5] Machado J. E., Ahmed S., Scherpen J. M. A. and Cucuzzella M., "Robust, distributed and optimal control of smart grids," *EPJ Web of Conferences*, **268** (2022) 00016.
[6] Lasseter R. and Paigi P., "Microgrid: a conceptual solution," in: *2004 IEEE 35th Annual Power Electronics Specialists Conference (IEEE Cat. No.04CH37551)*, Vol. **6**, pp. 4285–4290, (2004).
[7] Karimi H., Davison E. J. and Iravani R., "Multivariable servomechanism controller for autonomous operation of a distributed generation unit: Design and performance evaluation," *IEEE Trans. Power Syst.*, **25** (2010) 853.
[8] Parisio A., Rikos E. and Glielmo L., "A model predictive control approach to microgrid operation optimization," *IEEE Trans. Control Syst. Technol.*, **22** (2014) 1813.
[9] Cucuzzella M., Incremona G. P. and Ferrara A., "Decentralized sliding mode control of islanded AC microgrids with arbitrary topology," *IEEE Trans. Indust. Electron.*, **64** (2017) 6706.
[10] Trip S., Cucuzzella M., De Persis C., van der Schaft A. and Ferrara A., "Passivity-based design of sliding modes for optimal load frequency control," *IEEE Trans. Control Syst. Technol.*, **27** (2019) 1893.
[11] Trip S., Cucuzzella M., De Persis C., Ferrara A. and Scherpen J. M. A., "Robust load frequency control of nonlinear power networks," *Int. J. Control*, **93** (2020) 346.
[12] Cucuzzella M., Trip S., Ferrara A. and Scherpen J., "Cooperative voltage control in AC microgrids," in: *2018 IEEE Conference on Decision and Control (CDC)*, pp. 6723–6728, (2018).
[13] Silani A., Cucuzzella M., Scherpen J. M. A. and Yazdanpanah M. J., "Output regulation for load frequency control," *IEEE Trans. Control Syst. Technol.*, **30** (2022) 1130.
[14] Feng S., Cucuzzella M., Bouman T., Steg L. and Scherpen J. M. A., "An integrated human-cyber-physical framework for control of microgrids," *IEEE Trans. Smart Grid*, **14** (2023) 3388.
[15] Justo J. J., Mwasilu F., Lee J. and Jung J.-W., "AC-microgrids versus DC-microgrids with distributed energy resources: A review," *Renewable Sustainable Energy Rev.*, **24** (2013) 387.
[16] Flourentzou N., Agelidis V. G. and Demetriades G. D., "VSC-based HVDC power transmission systems: An overview," *IEEE Trans. Power Electron.*, **24** (2009) 592.
[17] Jeltsema D. and Scherpen J., "Tuning of passivity-preserving controllers for switched-mode power converters," *IEEE Trans. Automatic Control*, **49** (2004) 1333.
[18] Escobar G., van der Schaft A. J. and Ortega R., "A Hamiltonian viewpoint in the modeling of switching power converters," *Automatica*, **35** (1999) 445.

[19] Kosaraju K. C., Cucuzzella M., Scherpen J. M. A. and Pasumarthy R., "Differentiation and passivity for control of Brayton-Moser systems," *IEEE Trans. Automatic Control*, **66** (2021) 1087.

[20] Ferguson J., Cucuzzella M. and Scherpen J. M. A., "Increasing the region of attraction in DC microgrids," *Automatica*, **151** (2023) 110883.

[21] Zhao J. and Dörfler F., "Distributed control and optimization in DC microgrids," *Automatica*, **61** (2015) 18.

[22] Dragičević T., Lu X., Vasquez J. C. and Guerrero J. M., "DC microgrids—part i: A review of control strategies and stabilization techniques," *IEEE Trans. Power Electron.*, **31** (2016) 4876.

[23] Cucuzzella M., Rosti S., Cavallo A. and Ferrara A., "Decentralized sliding mode voltage control in DC microgrids," in: *2017 American Control Conference (ACC)*, pp. 3445–3450, (2017).

[24] Cucuzzella M., Lazzari R., Trip S., Rosti S., Sandroni C. and Ferrara A., "Sliding mode voltage control of boost converters in DC microgrids," *Control Engin. Practice*, **73** (2018) 161.

[25] Cucuzzella M., Lazzari R., Kawano Y., Kosaraju K. C. and Scherpen J. M. A., "Robust passivity-based control of boost converters in DC microgrids," in: *2019 IEEE 58th Conference on Decision and Control (CDC)*, pp. 8435–8440, (2019).

[26] Ferguson J., Cucuzzella M. and Scherpen J. M. A., "Exponential stability and local iss for DC networks," *IEEE Control Syst. Lett.*, **5** (2021) 893.

[27] Silani A., Cucuzzella M., Scherpen J. M. A. and Yazdanpanah M. J., "Output regulation for voltage control in DC networks with time-varying loads," *IEEE Control Syst. Lett.*, **5** (2021) 797.

[28] Silani A., Cucuzzella M., Scherpen J. M. A. and Yazdanpanah M. J., "Robust output regulation for voltage control in DC networks with time-varying loads," *Automatica*, **135** (2022) 109997.

[29] Cucuzzella M., Kosaraju K. C. and Scherpen J. M. A., "Voltage control of DC microgrids: Robustness for unknown ZIP-loads," *IEEE Control Syst. Lett.*, **7** (2023) 139.

[30] Fu Z., Cenedese C., Cucuzzella M., Kawano Y., Yu W. and Scherpen J. M. A., "Novel control approaches based on projection dynamics," *IEEE Control Syst. Lett.*, **7** (2023) 2179.

[31] Kawano Y., Moreschini A. and Cucuzzella M., "Krasovskii passivity for sampled-data stabilization and output consensus", preprint arXiv (2023).

[32] Monfared M. N., Kawano Y. and Cucuzzella M., "Voltage control of boost converters: Feasibility guarantees," *IFAC-PapersOnLine*, **56** (2023) 803, *22nd IFAC World Congress.*

[33] Malan A. J., Ferguson J., Cucuzzella M., Scherpen J. M. A. and Hohmann S., "Passivation of clustered DC microgrids with non-monotone loads", preprint arXiv (2024).

[34] Anand S., Fernandes B. G. and Guerrero J., "Distributed control to ensure proportional load sharing and improve voltage regulation in low-voltage DC microgrids," *IEEE Trans. Power Electron.*, **28** (2013) 1900.

[35] Nasirian V., Davoudi A., Lewis F. L. and Guerrero J. M., "Distributed adaptive droop control for DC distribution systems," *IEEE Trans. Energy Conversion*, **29** (2014) 944.

[36] Trip S., Han R., Cucuzzella M., Cheng X., Scherpen J. and Guerrero J., "Distributed averaging control for voltage regulation and current sharing in DC microgrids: Modelling and experimental validation," *IFAC-PapersOnLine*, **51** (2018) 242, *7th IFAC Workshop on Distributed Estimation and Control in Networked Systems, NECSYS 2018.*

[37] Cucuzzella M., Trip S. and Scherpen J., "A consensus-based controller for DC power networks," *IFAC-PapersOnLine*, **51** (2018) 205, *5th IFAC Conference on Analysis and Control of Chaotic Systems CHAOS 2018*.

[38] Zonetti D., Ortega R. and Schiffer J., "A tool for stability and power-sharing analysis of a generalized class of droop controllers for high-voltage direct-current transmission systems," *IEEE Trans. Control Network Syst.*, **5** (2018) 1110.

[39] Persis C. D., Weitenberg E. R. and Dörfler F., "A power consensus algorithm for DC microgrids," *Automatica*, **89** (2018) 364.

[40] Cucuzzella M., Trip S., De Persis C., Cheng X., Ferrara A. and van der Schaft A., "A robust consensus algorithm for current sharing and voltage regulation in DC microgrids," *IEEE Trans. Control Syst. Technol.*, **27** (2019) 1583.

[41] Trip S., Cucuzzella M., Cheng X. and Scherpen J., "Distributed averaging control for voltage regulation and current sharing in DC microgrids," *IEEE Control Syst. Lett.*, **3** (2019) 174.

[42] Cucuzzella M., Kosaraju K. C. and Scherpen J. M. A., "Distributed passivity-based control of DC microgrids," in: *2019 American Control Conference (ACC)*, pp. 652–657, (2019).

[43] Tucci M., Meng L., Guerrero J. M. and Ferrari-Trecate G., "Stable current sharing and voltage balancing in DC microgrids: A consensus-based secondary control layer," *Automatica*, **95** (2018) 1.

[44] Sahoo S. and Mishra S., "A distributed finite-time secondary average voltage regulation and current sharing controller for DC microgrids," *IEEE Trans. Smart Grid*, **10** (2019) 282.

[45] Prabhakaran P., Goyal Y. and Agarwal V., "A novel communication-based average voltage regulation scheme for a droop controlled DC microgrid," *IEEE Trans. Smart Grid*, **10** (2019) 1250.

[46] Kawano Y., Cucuzzella M., Feng S. and Scherpen J. M., "Krasovskii and shifted passivity based output consensus," *Automatica*, **155** (2023) 111167.

[47] Kawano Y., Cucuzzella M. and Scherpen J. M. A., "Krasovskii and shifted passivity approaches to mixed input/output consensus," *IEEE Control Syst. Lett.*, **7** (2023) 1951.

[48] Nasirian V., Moayedi S., Davoudi A. and Lewis F. L., "Distributed cooperative control of DC microgrids," *IEEE Trans. Power Electron.*, **30** (2015) 2288.

[49] Sadabadi M. S., Shafiee Q. and Karimi A., "Plug-and-play robust voltage control of DC microgrids," *IEEE Trans. Smart Grid*, **9** (2018) 6886.

[50] Strehle F., Pfeifer M., Malan A. J., Krebs S. and Hohmann S., "A scalable port-hamiltonian approach to plug-and-play voltage stabilization in DC microgrids," in: *2020 IEEE Conference on Control Technology and Applications (CCTA)*, pp. 787–794, (2020).

[51] Monshizadeh P., Machado J. E., Ortega R. and van der Schaft A., "Power-controlled hamiltonian systems: Application to electrical systems with constant power loads," *Automatica*, **109** (2019) 108527.

[52] Machado J. E., Ortega R., Astolfi A., Arocas-Pérez J., Pyrkin A., Bobtsov A. A. and Griñó R., "An adaptive observer-based controller design for active damping of a DC network with a constant power load," *IEEE Trans. Control Syst. Technol.*, **29** (2021) 2312.

[53] Dashkovskiy S. N. and Rüffer B. S., "Local iss of large-scale interconnections and estimates for stability regions," *Syst. Control Lett.*, **59** (2010) 241.

[54] Machado J. E., Rinaldi G., Cucuzzella M., Menon P. P., Scherpen J. M. and Ferrara A., "Online parameters estimation schemes to enhance control performance in DC microgrids," *Eur. J. Control*, **74** (2023) 100860.

[55] Kosaraju K. C., Cucuzzella M. and Scherpen J. M. A., "Distributed control of DC microgrids using primal-dual dynamics," in: *2019 IEEE 58th Conference on Decision and Control (CDC)*, pp. 6215–6220, (2019).
[56] Cucuzzella M., Bouman T., Kosaraju K. C., Schuitema G., Lemmen N. H., Johnson-Zawadzki S., Fischione C., Steg L. and Scherpen J. M. A., "Distributed control of DC grids: Integrating prosumers' motives," *IEEE Trans. Power Systems*, **37** (2022) 3299.
[57] Fu Z., Cucuzzella M., Cenedese C., Yu W. and Scherpen J. M. A., "A distributed control framework for the optimal operation of DC microgrids," in: *2022 IEEE 61st Conference on Decision and Control (CDC)*, pp. 4585–4590, (2022).